Large-scale pseudostate calculations for electron scattering from neon atoms

Oleg Zatsarinny and Klaus Bartschat

Phys. Rev. A **85**, 062710 — Published 27 June 2012

DOI: 10.1103/PhysRevA.85.062710

Large-scale pseudostate calculations for electron scattering from neon atoms

Oleg Zatsarinny and Klaus Bartschat
Department of Physics and Astronomy, Drake University, Des Moines, Iowa, 50311, USA
(Dated: June 1, 2012)

We report large-scale R-matrix (close-coupling) with pseudostates calculations for electron scattering from Ne atoms. The present calculations were performed in the nonrelativistic LS-coupling approximation with a recently developed parallel version of our suite of B-spline R-matrix codes. The principal goal was to generate converged (with the number of states in the close-coupling expansion) results for angle-integrated elastic, ionization, and total cross sections. The cross sections for excitation, which are also required for the latter, are generated in this nonrelativistic model as the sum for all terms. The close-coupling expansion used in this work includes 679 target states, with the lowest-lying 55 states representing the Ne bound spectrum and the remaining 624 states representing the ionization continuum. Our results are in close agreement with available experimental data for the elastic and total cross sections over the wide range of electron energies between 0.1 eV and 200 eV. With the pseudostate approach, we also obtain accurate cross sections for ionization from both the ground and the metastable states of neon. Our results confirm the very strong influence of coupling to the target continuum on theoretical predictions for excitation cross sections in Ne at intermediate energies, an effect that was previously reported by Ballance and Griffin [J. Phys.B **37**, 2943 (2004)].

PACS numbers: 34.80.Bm, 34.80.Dp

I. INTRODUCTION

Electron collisions with neon atoms are well known to be important for both fundamental as well as practical reasons. The latter include modeling applications in the lighting and laser industry [1, 2], plasma processing [3, 4], and the interpretation of astrophysical data [5, 6]. Not surprisingly, therefore, significant experimental and theoretical efforts have been devoted to this system for many years.

From a theoretical point of view, neon can be regarded as a relatively light target with the ground state represented as a compact closed-shell system. Consequently, it was a particularly favorable target for developing and testing collision models for elastic scattering. Indeed, in the elastic regime of collision energies below the first excitation threshold of 16.62 eV for the $(2p^5 3s)^3P_2$ state (also denoted as $3s[3/2]_2$ or $1s_5$), polarized-orbital approaches (see, for example, [7–9]), were highly successful, except for the description of the $(2p^5 3s^2)^2P_{3/2,1/2}$ Feshbach resonances just below this threshold. The principal challenge in such calculations is a good description of the polarization of the atomic charge cloud, especially when the projectile is moving slowly. These effects can also be described well in specially designed close-coupling approaches, in which the dipole polarizability of the ground state is represented through coupling to "pseudostates" with ${}^1P^o$ symmetry [10], which are of significantly shorter range than the corresponding physical states.

For excitation processes, on the other hand, the situation is much less satisfactory. As shown, for example, by Khakoo *et al.* [11], none of the many theoretical methods was able to consistently reproduce the experimental data for angle-differential cross sections for excitation of the $2p^5 3s$ states, or their ratios, which represent a very sensitive test of the quality of the theoretical model.

In the low-energy region below the ionization threshold, however, significant progress has recently been made by means of the B-spline R-matrix (BSR) method. Excellent agreement with experiment was observed, for instance, for the calculated energy-dependent cross sections for the production of metastable Ne atoms [12]. The predicted resonance structure was subsequently confirmed experimentally [13]. Very good agreement at low energies was also achieved for the energy-dependent differential cross sections for excitation of the $2p^5 3s$ and $2p^5 3p$ states [14, 15]. The key feature of the BSR method and the published suite of computer codes [16] is the possibility to employ *nonorthogonal* sets of term-dependent one-electron orbitals. This allows us to generate much more accurate target descriptions compared to earlier calculations that are limited to a single set of orthogonal orbitals.

Despite the fact that the previous BSR calculations [12–15] very accurately reproduced the low-energy near-threshold resonance structure, they did not account for coupling to the target continuum. Consequently, they cannot be considered fully converged regarding, for example, the absolute values of the excitation cross sections. The problem is particularly imminent for neutral and low-charge-state species at intermediate energies ranging from about one to five times the ionization threshold, as well as for optically forbidden transitions, which are often associated with relatively small cross sections. The effects of coupling to the target continuum on theoretical predictions for electron impact excitation have been demonstrated convincingly in many advanced close-coupling calculations, most frequently based on the convergent close-coupling (CCC) [17] method formulated in momentum space or the R-matrix with pseudostates (RMPS) [18, 19] approach in coordinate space.

In the specific case of the e-Ne collision system, the problem was demonstrated by Ballance and Griffin [20]. They showed that the effects of continuum coupling may reduce the theoretical cross section by factors up to five. Most surprisingly, this included the strong dipole transition from the $(2p^6)^1S$ ground state to the $(2p^5 3d)^1P$ state. While never confirmed by another calculation or a direct state-selective crossed-beam experiment, detailed modeling of the Ne lines seen in a plasma discharge [21] provided some indirect support for the findings of Ballance and Griffin.

Along with elastic scattering and excitation, ionization processes are very important in plasma modeling. The pseudostate approach, employed in the present work, allows for a straightforward calculation of total ionization cross sections by summing up the excitation cross sections for all the continuum pseudostates. This can be done for any initial state. In practice, ionization from the ground state and the metastable states are most important. The cross sections for the latter are significantly larger than those for the former, in particular at low projectile energies. Hence, the small but appreciable population of the metastable excited states relative to the ground state in many laboratory and astrophysical plasmas is compensated by the large cross sections. Ionization of metastable atoms and ions, therefore, may even dominate the effective ionization rate.

The purpose of the present calculations is fourfold. To begin with, we perform an independent check of the continuum coupling effects predicted by Ballance and Griffin [20], using even more extensive pseudostate expansions that reflect the rapid development in computational facilities in recent years. Furthermore, we generate benchmark results including all the important processes in e-Ne collisions over a wide range of projectile energies. Next, the present work is an important stepping stone to a (semi)relativistic model. Such a model is necessary in order to obtain reliable state-specific cross sections for excitation of the many states in Ne that cannot be described properly by an LS-coupling scheme. And, finally, using a large number of densely spaced pseudostates will allow us to use this model also for the calculation of energy- and angle-differential ionization processes, similar to what we recently did for helium [22] and argon [23].

This paper is organized as follows. In Section II we describe the computational model, specifically for the target structure (II.A) and the collision calculations(II.B). This is followed by results for elastic scattering, excitation, ionization, and total cross sections in Section III. In addition to the angle-integrated cross sections, we also present some comparisons with experiment and other theories for angle-differential elastic scattering in Section III.A. We finish with a brief summary and an outlook in Section IV.

II. COMPUTATIONAL DETAILS

A. Structure calculations

The target states of neon in the present calculations were generated by combining the multi-configuration Hartree-Fock (MCHF) and the B-spline box-based close-coupling methods [24]. Specifically, the structure of the multi-channel target expansion was chosen as

$$\begin{aligned}\Phi(2s^2 2p^6 nl, LS) &= \sum_{nl} \left\{\phi(2s^2 2p^5) P(nl)\right\}^{LS} \\ &+ \sum_{nl} \left\{\phi(2s 2p^6) P(nl)\right\}^{LS} \\ &+ a\varphi(2s^2 2p^6)^1 S, \end{aligned} \quad (1)$$

where $P(nl)$ denotes the orbital of the outer valence electron, while the ϕ and φ functions represent the configuration interaction (CI) expansions of the corresponding ionic or specific atomic states, respectively. These expansions were generated in separate MCHF calculations for each state using the MCHF program [25].

The expansion (1) can be considered a model for the entire $2s^2 3p^5 nl$ and $2s 2p^6 nl$ Rydberg series of bound states in Ne, including the continuum pseudostates lying above the ionization limit. Although this expansion can also provide a good approximation for the ground state, we chose to use a separate CI expansion for this state by directly including relaxation effects via state-specific one-electron orbitals. Inner-core (short-range) correlation is accounted for through the CI expansion of the ionic states. These expansions include all single and double excitations from the $2s$ and $2p$ orbitals to the $3l$ and $4l$ (l=0-3) correlated orbitals. These orbitals were generated for each state separately. To keep the final expansions for the atomic states to a reasonable size, all CI expansions were restricted by dropping contributions with coefficients whose magnitude was less than the cut-off parameter of 0.02. The resulting ionization potentials for the two ionic states $2s^2 2p^5$ and $2s 2p^6$ agreed with experiment [26] to within 0.05 eV.

The unknown functions $P(nl)$ for the outer valence electron were expanded in a B-spline basis, and the corresponding equations were solved subject to the condition that the orbitals vanish at the boundary. The B-spline coefficients for the valence electron orbitals $P(nl)$, along with the coefficient a for the ground state, were obtained by diagonalizing the atomic Hamiltonian in the non-relativistic LS-approximation. Since the B-spline bound-state close-coupling calculations generate different non-orthogonal sets of orbitals for each atomic state, their subsequent use is somewhat complicated. Our configuration expansions for the atomic target states contained at most 60 configurations for each state. These could still be used in the subsequent large-scale collision calculations with our currently available computational resources.

B. Scattering calculations

Our close-coupling expansion includes 679 states of neon, with 55 states representing the bound spectrum and the remaining 624 the target continuum. We included all singlet and triplet target states with total electronic angular momentum $L = 0 - 4$. The continuum pseudostates in the present calculations cover the energy region up to 85 eV. This model will be referred to as BSR-679 below. As mentioned above, the present calculation is also a stepping stone towards the treatment of ionization processes. With this range of pseudostate energies, we should be able to model an ongoing experiment of the Heidelberg group [27].

The close-coupling equations were solved by means of the R-matrix method, using a parallelized version of the BSR complex [16]. The distinctive feature of the method is the use of B-splines as a universal basis to represent the scattering orbitals in the inner region of $r \leq a$. Hence, the R-matrix expansion in this region takes the form

$$\Psi_k(x_1, \ldots, x_{N+1}) = \mathcal{A} \sum_{ij} \bar{\Phi}_i(x_1, \ldots, x_N; \hat{\mathbf{r}}_{N+1}\sigma_{N+1})\, r_{N+1}^{-1}\, B_j(r_{N+1})\, a_{ijk} + \sum_i \chi_i(x_1, \ldots, x_{N+1})\, b_{ik}. \quad (2)$$

Here the $\bar{\Phi}_i$ denote the channel functions constructed from the N-electron target states and the angular and spin coordinates of the projectile, while the splines $B_j(r)$ represent the radial part of the continuum orbitals. The χ_i are additional $(N+1)$-electron bound states. In standard R-matrix calculations [28], the latter are included one configuration at a time to ensure completeness of the total trial wave function and to compensate for orthogonality constraints imposed on the continuum orbitals. The use of nonorthogonal one-electron radial functions in the BSR method, on the other hand, allows us to avoid these configurations for compensating orthogonality restrictions. In the present calculations the bound channels were completely omitted.

The R-matrix radius was set to $30\,a_0$, where $a_0 = 0.529 \times 10^{-10}\,\mathrm{m}$ is the Bohr radius. We employed 70 B-splines to span this radial range using a semi-exponential knot grid. The maximum interval in this grid is $0.5\,a_0$. This is sufficient to cover electron scattering energies up to 200 eV. The present scattering model contained up to 2,280 scattering channels, leading to generalized eigenvalue problems with matrix dimensions up to 150,000 in the B-spline basis. Matrices of such dimensions can be handled with our current computational resources. We calculated partial waves for total orbital angular momenta $L \leq 25$ numerically and then used a top-up procedure to estimate the contribution to the cross sections from even higher L values. The calculation for the external region was performed using the STGF program [29].

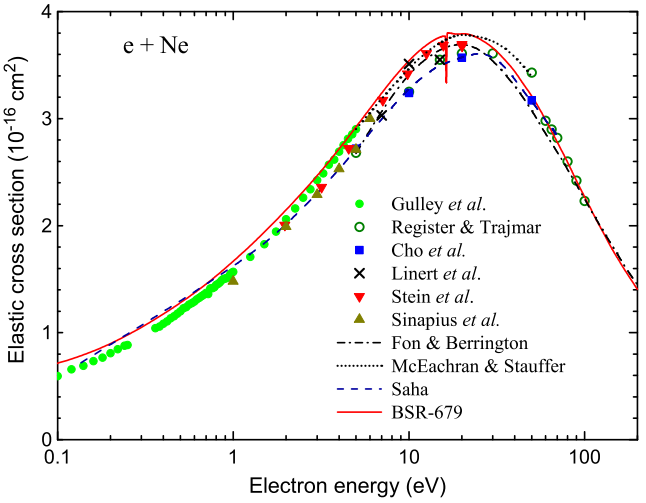

FIG. 1: (Color online) Angle-integrated elastic cross section for electron scattering from neon. The current BSR-679 predictions are compared with experimental data from Stein *et al.* [31], Sinapius *et al.* [32], Register and Trajmar [33], Gulley *et al.* [34], Linert *et al.* [35], and Cho *et al.* [36], and with theoretical results from Fon and Berrington [10], McEachran and Stauffer [7], and Saha [8].

III. RESULTS

A. Elastic scattering

For low-energy elastic scattering, it is very important to account for the full dipole polarizability of the ground state. Our close-coupling expansion yields a polarizability of $2.673\,a_0^3$, which is very close to the experimental value of $2.670 \pm 0.005\,a_0^3$ [30]. Since the largest part of this polarization originates from coupling to the continuum pseudostates, this result confirms the effective completeness of our basis in this regard.

Figure 1 exhibits results for the angle-integrated elastic cross section (ICS) for e−Ne-scattering, showing overall good agreement with available experimental data over the wide range of incident energies from 0.1 to 200 eV. We compare our results with those from early calculations using a two-state (ground state plus one specially designed pseudostate) R-matrix model by Fon and Berrington [10], a polarized-orbital approach by McEachran and Stauffer [7], and an MCHF approach with dynamic polarization by Saha [8]. On average, our results are about 5-10% higher than other theoretical predictions, with the closest agreement seen to the polarized-orbital calculations [7].

Note that all these previous calculations were specially designed, and hence also limited, to treat the elastic scattering problem, whereas our calculations handle excitation and ionization processes as well. Our model also reproduces the strong $(2p^5 3s^2)^2 P^o$ Feshbach resonance just above 16 eV incident energy. For a detailed discussion of this and other resonances in the e−Ne collision problem (obtained using the appropriate intermediate

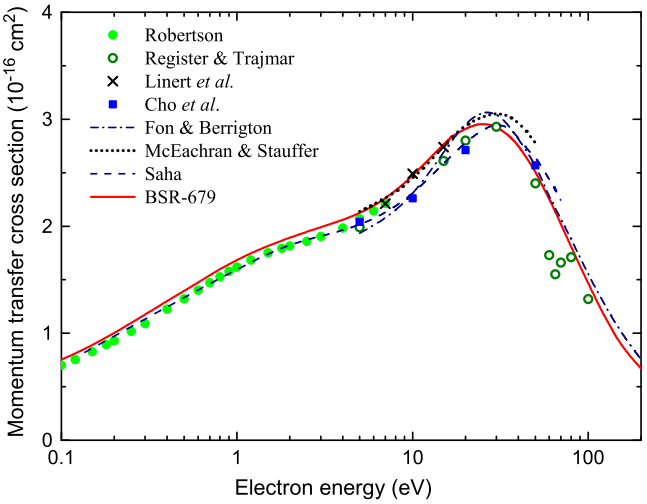

FIG. 2: (Color online) Elastic momentum transfer cross section for e−Ne collisions. The current BSR-679 predictions are compared with experimental data from Robertson [37], Register and Trajmar [33], Linert *et al.* [35], and Cho *et al.* [36], and with theoretical results from Fon and Berrington [10], McEachran and Stauffer [7], and Saha [8].

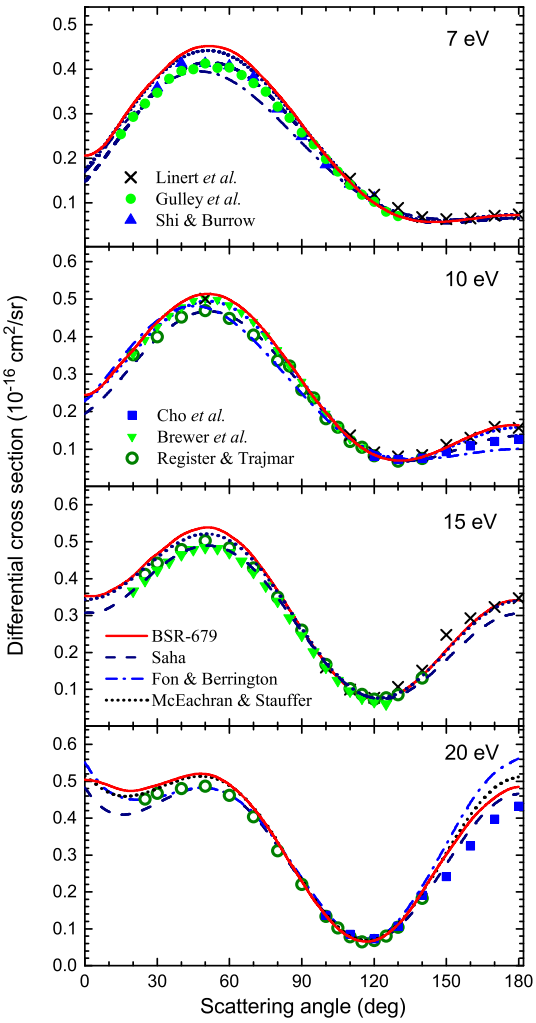

FIG. 3: (Color online) Angle-differential cross section for elastic electron scattering from neon. The current BSR-679 predictions are compared with experimental data from Linert *et al.* [35], Gulley *et al.* [34], Shi and Burrow [38], Brewer *et al.* [39], Register and Trajmar [33], and Cho *et al.* [36], and theoretical results from Fon and Berrington [10], McEachran and Stauffer [7], and Saha [8].

coupling scheme), we refer to our previous paper [13].

Figure 2 compares the present values of the momentum transfer cross sections (MTCS) with available experimental data and a selection of other theoretical results. For energies below 7 eV, our cross sections are within 5% of the values reported by Robertson [37]. For higher energies above 25 eV, our values are in close agreement with the measurements of Register and Trajmar [33] at all energies, except for 60 eV, 65 eV, and 75 eV, where the experimental data exhibit significant scatter that lies well outside the expected energy dependence. At intermediate energies, we obtain excellent agreement with the measurements of Linert *et al.* [35], whereas the most recent measurements of Cho *et al.* [36] are 10% lower at 10 eV and 20 eV.

It is worth noting that "experimentally" determined ICS and MTCS results often include theoretical predictions for the angular range that is not accessible to actual measurements of the elastic angle-differential cross section (DCS). Regarding the comparison with other theories, we obtain once again the best agreement with the polarized-orbital calculations by McEachran and Stauffer [7], albeit noticeable differences can be seen at higher energies.

A sample of DCS results for elastic scattering from neon is given in Fig. 3. From the large database of available cross sections in the literature, we select for comparison the energies from the most recent experiments [35, 36], where the measurements were extended to backward angles up to 180°. At 7 eV, all theoretical results presented here are in very good agreement in the backward region with the measurements of Linert *et al.* [35]. At the DCS maximum around 50°, however, the calculations differ by up to 15%, and once again we agree best with the polarized-orbital calculations of McEachran and Stauffer [7]. At 10 eV, our results and the polarized-orbital calculations [7] again agree well with the measurements by Linert *et al.* [35] in the backward regime. The results of Saha [8] and in particular those of Fon and Berrington [10] are considerably smaller, and hence they agree closely with the measurements of Cho *et al.* [36]. At 15 eV, there is again good agreement between our calculations and the measurements of [35], while all presented calculations lie well above the experimental data of Cho *et al.* [36] for 20 eV. Overall, the comparison shows that the present BSR-679 calculations reproduce the existing experimental DCSs accurately for all scattering angles, yielding considerable improvement over our previous 31-

state BSR model. The latter calculations were discussed in [35] and are not presented here in the interest of clarity in the figures.

B. Excitation

Figure 4 exhibits selected nonrelativistic results for excitation of LS-coupled terms. They were chosen in order to discuss the convergence of the close-coupling expansion for e−Ne collisions. These results cannot be directly compared to experiment, since most Ne target states should be described at least in a semirelativistic intermediate-coupling scheme involving several terms. Nevertheless, we can compare our predictions with the RMPS results of Ballance and Griffin [20], who performed both a standard 61-term R-matrix calculation (RM-61)with only discrete terms included in the close-coupling expansion and a 243-term RMPS calculation (RMPS-243).

The results of these calculations for excitation of the $(2p^5 3s)^3P$ and $(2p^5 3s)^1P$ terms are shown in the top panels of Fig. 4. The striking differences between the 61-term and the 243-term results clearly demonstrate the significance of continuum coupling effects. These effects have a pronounced influence on the theoretical cross sections, especially above the ionization limit, where the discrete-term-only RM-61 cross section is a factor of two larger than the RMPS-243 cross section at 30 eV for excitation of the $(2p^5 3s)^3P$ term and a factor of 1.5 larger at 32 eV for excitation of the $(2p^5 3s)^1P$ term. Our even more extended BSR-679 calculation produces results slightly below the RMPS-243 numbers. This may not just be due to additional channel coupling, but also to differences in the atomic wave functions from the respective structure models. Overall, however, we conclude that the pseudostate expansion in the RMPS-243 model is already sufficiently complete to yield reliable cross sections.

The panels in the center row of Fig. 4 show the corresponding comparisons for excitation from the ground state to the $(2p^5 3p)^3S$ and $(2p^5 3p)^3D$ terms, respectively. At 30 eV, continuum coupling reduces both cross sections by more than a factor of two, and these effects persist even below the ionization limit. Our BSR-679 results suggest even smaller cross sections than the RMPS-243 model [20].

Finally, the bottom panels of Fig. 4 compare predictions for excitation of the $(2p^5 3d)^3P$ and $(2p^5 3d)^1P$ terms from the ground state. The effects of continuum coupling are very large for both cases. Most surprisingly, even for the relatively strong dipole-allowed $(2p^6)^1S \rightarrow (2p^5 3d)^1P$ transition, they cause a huge reduction of the calculated cross section by nearly a factor of 5 at 40 eV. The present 679-state calculation completely supports the findings of Ballance and Griffin [20], and we see very close agreement between the BSR-679 and RMPS-243 results. Hence, we conclude that the remaining differences in the target wave functions are not very important here, and that both the RMPS and BSR expansions are sufficiently complete to describe these transitions. Recall that there is also further, albeit indirect, evidence that discrete-state-only calculations such as our original BSR-31 model may significantly overestimate the cross sections for excitation of states with dominant configuration $2p^5 3d$ [21].

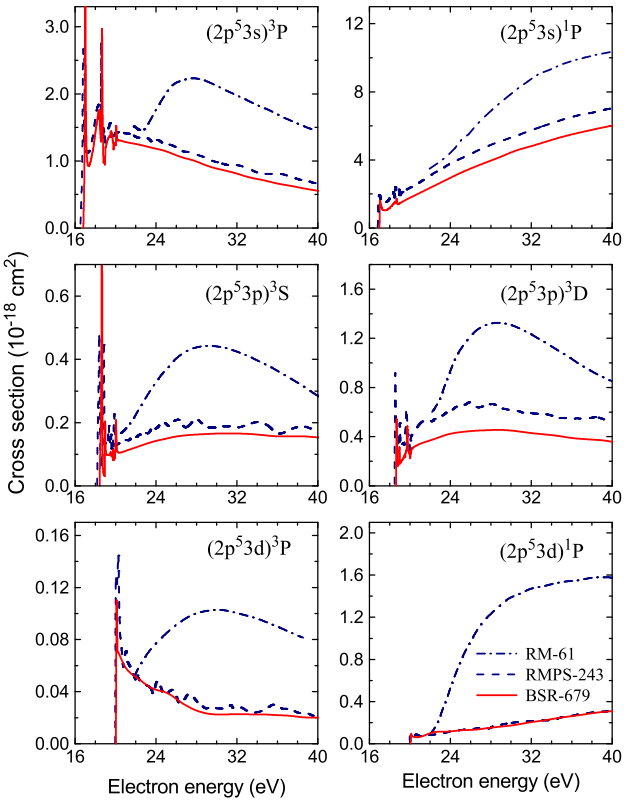

FIG. 4: (Color online) LS-coupling results for electron impact excitation cross sections from the $(2p^6)^1S$ ground state of neon to the $(2p^5 3s)^{3,1}P$ (top row), $(2p^5 3p)^3S$ and $(2p^5 3p)^3D$ (center row), and $(2p^5 3d)^{3,1}P$ (bottom row) terms. The current BSR-679 predictions are compared with the 61-state and 243-state results of Ballance and Griffin [20].

As mentioned above, the intermediate-coupling nature of the Ne target states does not allow for a direct comparison with experimental data for excitation of individual states. However, the above results give us confidence in extending the calculations to a semirelativistic Breit-Pauli description. While the computational effort will further increase significantly, such calculations can now be handled on state-of-the-art supercomputers. Initial results are promising, and state-selective excitation cross sections obtained in the intermediate-coupling scheme will be presented in a separate publication in the near future.

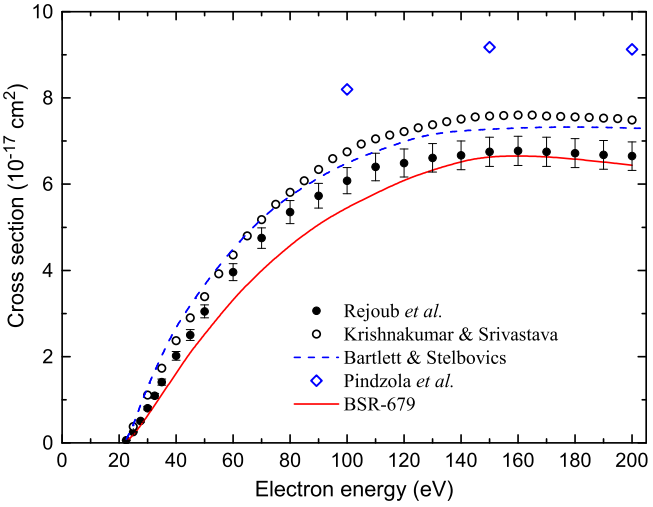

FIG. 5: (Color online) Cross section for electron impact ionization of the Ne $(2s^2 2p^6)^1S$ ground state. The current BSR-679 predictions are compared with the experimental data of Krishnakumar and Srivastava [42] and of Rejoub *et al.* [43], as well as the theoretical results of Pindzola *et al.* [44] and of Bartlett and Stelbovics [45].

C. Ionization

The reliable description of electronimpact single ionization of a complex atom or ion remains a formidable theoretical and computational challenge. One of the most widely used quantal methods for treating direct ionization of arbitrary atoms and ions has been the application of first-order perturbation theory using distorted waves. Recently, fully *ab initio* quantal nonperturbative methods have been developed and applied to the direct ionization of one-electron (hydrogen-like) and two-electron (helium-like) atoms and ions. These methods include grid-based approaches such as exterior complex scaling (ECS) [40] and time-dependent close-coupling (TDCC) [41], as well as the aforementioned CCC approach [17]. Extension of these methods to more complex targets (beyond model potentials to represent closed cores in quasi-one and quasi-two electron systems) has not been achieved to date, mostly due to the lack of a proper interface between these collision models and the sophisticated structure codes needed for such problems. Consequently, the RMPS method – either in the standard form based on the Belfast suite of R-matrix codes [18, 19] or in the present BSR implementation – remains the most frequently used tool for a nonperturbative treatment of ionization processes in complex atoms. The ongoing rapid development of modern computational facilities often allows for the inclusion of a sufficiently large number of pseudostates to accurately model ionization processes.

In the RMPS approach, the ionization process is treated as excitation of the continuum pseudostates. Figure 5 compares our total ionization cross sections with experimental data and a few other selected theoretical predictions. Our results are closest to the recent measurements by Rejoub *et al.* [43], but they still differ from the experimental values by 15-20% at intermediate energies between about 40 eV and 120 eV. We first calculated the ionization cross section by the straightforward method of adding the cross sections for all pseudostates lying above the ionization threshold. We then calculated the ionization amplitude by direct projection of the pseudostates to the proper continuum wavefunction of the ejected-electron–residual-ion system [22, 23] and numerically integrated the triple-differential cross section. The results from the two approaches differed by less than 2% and give us confidence in the numerical accuracy and consistency of our approach. Nevertheless, a possible reason for the discrepancy might be a still insufficient density of pseudostates in the present model. By using a larger R-matrix radius, we could gradually increase the density of the continuum pseudostates. Further tests are planned, but the present calculations are already very expensive, and we are simply restricted by the available computational facilities. Unfortunately, neither Ballance and Griffin [20] nor Ballance *et al.* [47] present ionization cross sections for the ground state.

As seen from Fig. 5, good agreement with experiment was also obtained in the much simpler Born-type calculations by Bartlett and Stelbovics [45]. The authors explain this somewhat surprising agreement by noting that considerable averaging over exchange and correlation effects occurs for the noble gases at lower energies, thereby enabling their Born model to provide good estimates for the total ionization cross sections. An attempt to obtain e−Ne ionization cross sections in the nonperturbative TDCC approach was made by Pindzola *et al.* [44]. As seen from the figure, the TDCC results are substantially higher than experiment at the peak of the cross section. According to the authors, the principal reason for the significant discrepancies with experiment is likely the use of very simple configuration-averaged target orbitals for the active electron.

The present pseudostate approach also allows for a straightforward extension to the calculation of cross sections for ionization from metastable excited levels. These calculations, however, are computationally more challenging in comparison to ionization from the ground state, due to additional partial-wave symmetries involved and the overall slower convergence of the partial-wave expansion because of the smaller threshold energy.

Figure 6 exhibits the present BSR cross sections for ionization from the $(2p^5 3s)^3P$ metastable term of neon, compared to the experimental data of Johnston *et al.* [46] and to RMPS calculations by Ballance *et al.* [47]. We see good agreement between experiment and the BSR-679 cross sections over a wide range of energies from threshold to 160 eV. There is also close agreement with the RMPS-243 results in the near-threshold energy region below 25 eV, where these results are available.

The theoretical results clearly fall within the error bars

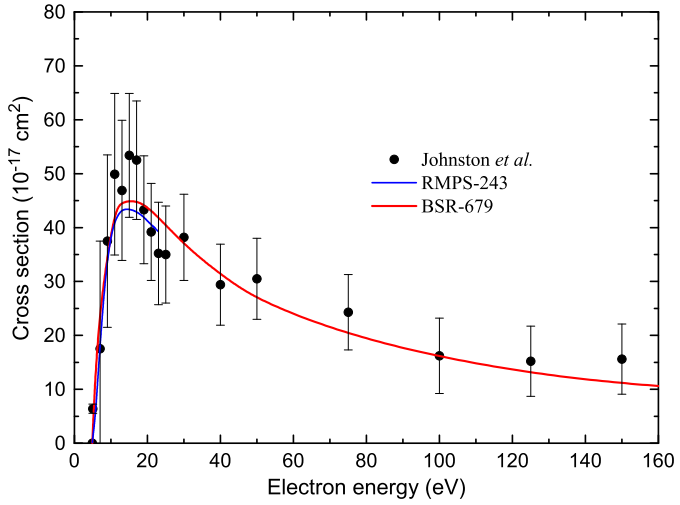

FIG. 6: (Color online) Cross section for electron impact ionization of the Ne $(2p^5 3s)^3P$ metastable state. The current BSR-679 predictions are compared with the experimental data of Johnston *et al.* [46] and the 243-state results of Ballance *et al.* [47].

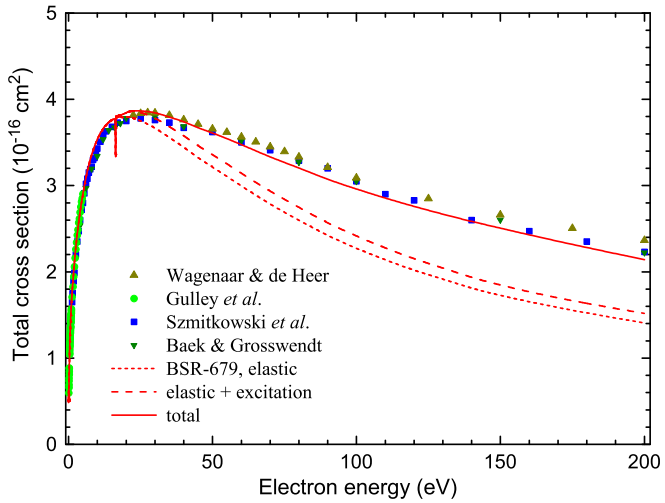

FIG. 7: (Color online) Total cross section for electron scattering from neon. The current BSR-679 predictions for elastic scattering alone, elastic scattering plus excitation, and Wagenaar and de Heer [48], Gulley *et al.* [34], Szmytkowski *et al.* [49], and Baek and Grosswendt [50].

of the experimental data. The size of these error bars, however, makes it difficult to judge the overall agreement. On the other hand, such a close agreement between two entirely independent pseudostate calculations suggests that the present metastable ionization cross section are sufficiently accurate to be used in collisional radiative modeling studies of neon plasmas.

D. Total cross section

Figure 7 finally compares our total (elastic + excitation + ionization) cross sections with a number of experimental data. We draw special attention to the higher energies, where ionization processes become increasingly important. The figure also shows the relative importance of the contributions from individual collision processes. Elastic scattering dominates over the entire energy regime shown in the figure. Excitation processes, on the other hand, only provide a relatively small contribution to the total cross section, while ionization becomes more and more important with increasing projectile energy and makes up nearly 30% of the total cross section at 200 eV. The overall excellent agreement with the available experimental data confirms the accuracy of the present approach. Indirectly, the results once again also support our ionization calculations.

IV. SUMMARY

We carried out large-scale R-matrix with pseudostates calculations for electron scattering on neon. The present results form a comprehensive study of all important electroninduced collision processes (elastic scattering, excitation, and ionization) in neon. They are based on first principles and use a *single* theoretical model to cover a wide range of incident electron energies between 0.1 eV and 200 eV.

The calculations were carried out with a recently developed parallel version of the BSR suite of computer programs. This paper exhibits the first results from these calculations, which were performed in the nonrelativistic LS-coupling scheme and are intended to provide converged cross sections for elastic scattering, the sum of all excitation processes, ionization, and the grand total cross section.

Our results confirm an earlier prediction [20] regarding a very strong influence of coupling to the target continuum in calculating excitation cross section for Ne, even for dipole-allowed transitions. The results show close agreement with available experimental data for both the elastic and the total cross sections. The remaining 15-20% disagreement with the experimental ionization cross sections at intermediate energies may be attributed to the density of the pseudostates in the current model and will be checked further when even larger calculations than the present ones will become possible. We also obtained good agreement with experiment for the ionization cross sections from the metastable states of neon.

The present approach is also capable to generate differential cross sections, which are more sensitive to the details of the scattering model. Our results for the elastic DCS at low energies are in excellent agreement with those from the polarized-orbital calculations of McEachran and Stauffer [7] and the experimental data of Linert *et al.* [35].

In the future, we plan to perform extensive pseudostate

calculations in the semirelativistic Breit-Pauli approach. This will allow us to produce state-selective cross sections for electron impact excitation, which will be reported in a separate publication. We will also continue to generate angle-differential results for both excitation and ionization processes.

Acknowledgments

This work was supported by the United States National Science Foundation under grants PHY-0757755, PHY-0903818, and the XSEDE supercomputer allocation TG-PHY090031. All calculations were carried out on Ranger and Lonestar at the Texas Austin Computer Center. Additional support from Drake University through a Troyer Research Fellowship (K.B.) is also gratefully acknowledged.

[1] V. Puech and S. Mizzi, J. Phys. D **24**, 1974 (1991).
[2] B. S. Gray, I. D. Latimor, and S. P. Spoor, J. Phys. D **29**, 50 (1996).
[3] S. A. Moshkalyov, P. G. Stenn, S. Gomez, and W. G. Graham, Appl. Phys. Lett. **75**, 328 (1999).
[4] M. V. Malyshev, V. M. Donnelly, and S. Samukawa, J. Appl. Phys. **84**, 1222 (1998).
[5] P. H. Hauschildt, S. Starrfield, S. M. Shore, F. Allard, and E. Naron, Astrophys. J. 447, 829 (1995).
[6] I. Kanik, J. M. Ajello, and G. K. James, J. Phys. B **29**, 2355 (1996).
[7] R. P. McEachran and A. D. Stauffer, J. Phys. B **16**, 4023 (1983).
[8] H. P. Saha, Phys. Rev. A **39**, 5048 (1989).
[9] A. Dasgupta and A. K. Bhatia, Phys. Rev. A **30**, 1241 (1984).
[10] W. C. Fon and K. A. Berrington, J. Phys. B **14**, 323 (1981).
[11] M. A. Khakoo *et al.*, Phys. Rev. A **65**, 062711 (2002).
[12] O. Zatsarinny and K. Bartschat, J. Phys. B **37**, 2173 (2004).
[13] J. Bömmels *et al.*, Phys. Rev. A **71**, 012704 (2005)
[14] M. Allan, O. Zatsarinny, and K. Bartschat, Phys. Rev. A **74**, 030701 (2006).
[15] M. Allan, K. Franz, H. Hotop, O. Zatsarinny, and K. Bartschat, J. Phys. B **42**, 044009 (2009).
[16] O. Zatsarinny, Comp. Phys. Commun. **174**, 273 (2006).
[17] I. Bray, D. V. Fursa, A. Kheifets, and A. T. Stelbovics, J. Phys. B **35** (2002) R117.
[18] K. Bartschat, E. T. Hudson, M. P. Scott, P. G. Burke, and V. M. Burke, J. Phys. B **29**, 115 (1996).
[19] K. Bartschat, E. T. Hudson, M. P. Scott, P. G. Burke, and V. M. Burke, Phys. Rev. A **54**, R998 (1996).
[20] C. P. Ballance and D. C. Griffin, J. Phys. B **37**, 2943 (2004).
[21] D. Dodt, A. Dinklage, K. Bartschat, and O. Zatsarinny, New Journal of Physics **12**, 073018 (2010).
[22] O. Zatsarinny and K. Bartschat, Phys. Rev. Lett. **107**, 023203 (2011).
[23] O. Zatsarinny and K. Bartschat, Phys. Rev. A **85**, 032708 (2012).
[24] O. Zatsarinny and C. Froese Fischer, Comp. Phys. Commun. **180**, 2041 (2009).
[25] C. Froese Fischer, Comp. Phys. Commun. **176**, 559 (2007).
[26] `http://physics.nist.gov/cgi-bin/AtData`.
[27] X. Ren and A. Dorn, *private communication* (2012).
[28] P. G. Burke, *R-Matrix Theory of Atomic Collisions*, Springer-Verlag (Berlin, Heidelberg 2011)
[29] N. Badnell, J. Phys. B **32**, 5583 (1999); see also `http://amdpp.phys.strath.ac.uk/UK_RmaX/codes.html`
[30] R. H. Orcutt, and R. H. Cole, J. Chem. Phys. **46**, 697 (1967).
[31] T. S. Stein, W. E. Kauppila, V. Pol, J. H. Smart, and G. Jesion, Phys. Rev. A **17**, 1600 (1978).
[32] G. Sinapius, W. Raith, and W. G. Wilson, J. Phys. B **13**, 4079 (1980).
[33] D. F. Register and S. Trajmar, Phys. Rev. A **29**, 1785 (1984).
[34] R. J. Gulley, D. T. Alle, M. J. Brennan, M. J. Brunger, and S. J. Buckman, J. Phys. B **27**, 2593 (1994).
[35] I. Linert, B. Mielewska, G. C. King, and M. Zubek, Phys. Rev. A **74**, 042701 (2006).
[36] H. Cho, R. P. McEachran, S. J. Buckman, and H. Tanaka, Phys. Rev. A **78**, 034702 (2008).
[37] A. G. Robertson, J. Phys. B **5**, 648 (1972).
[38] X. Shi and P. D. Burrow, J. Phys. B **25**, 4723 (1992).
[39] D. F. C. Brewer, W. R. Newell, S. F. W. Harper, and A. C. H. Smith, J. Phys. B **14**, L749 (1981).
[40] T. N. Rescigno, M. Baertschy, W. A. Isaacs, and C. W. McCurdy, Science **286** (1999) 2474.
[41] J. Colgan, M. S. Pindzola, F. J. Robicheaux, D. C. Griffin, and M. Baertschy, Phys. Rev. A **65** (2002) 042721.
[42] E. Krishnakumar and S. K. Srivastava, J. Phys. B **21**, 1055 (1988).
[43] R. Rejoub, B. G. Lindsay, and R. F. Stebbings, Phys. Rev. A **65**, 042713 (2002).
[44] M. S. Pindzola, J. Colgan, F. Robicheaux, and D. C. Griffin, Phys. Rev. A **62**, 042705 (2000).
[45] P. L. Bartlett and A. T. Stelbovics, Phys. Rev. A **66**, 012707 (2002).
[46] M. Johnston, K. Fujii, J. Nickel, and S. Trajmar, J. Phys. B **29**, 531 (1996).
[47] C. P. Ballance, D. C. Griffin, J. A. Ludlow, and M. S. Pindzola, J. Phys. B **37**, 4779 (2004).
[48] R. W. Wagenaar and F. J. de Heer, J. Phys. B **13**, 3855 (1980).
[49] C. Szmytkowski, K. Maciag, and G. Karwasz, Physica Scripta **54**, 271 (1996).
[50] W. Y. Baek and B. Grosswendt, J. Phys. B **36**, 731 (2003).